



mDSF: Improved Fuel Efficiency, Drivability and Vibrations via Dynamic Skip Fire and Miller Cycle Synergies

Elliott Ortiz-Soto, Benjamin Wolk, Hao Chen, and Matthew Younkins Tula Technology, Inc.

Citation: Ortiz-Soto, E., Wolk, B., Chen, H., and Younkins, M., "mDSF: Improved Fuel Efficiency, Drivability and Vibrations via Dynamic Skip Fire and Miller Cycle Synergies," SAE Technical Paper 2019-01-0227, 2019, doi:10.4271/2019-01-0227.

Abstract

mDSF is a novel cylinder deactivation technology developed at Tula Technology, which combines the torque control of Dynamic Skip Fire (DSF) with Miller cycle engines to optimize fuel efficiency at minimal cost. mDSF employs a valvetrain with variable valve lift plus deactivation and novel control algorithms founded on Tula's proven DSF technology. This allows cylinders to dynamically alternate among 3 potential states: high-charge fire, low-charge fire, and skip (deactivation). The low-charge fire state is achieved through an aggressive Miller cycle with Early Intake Valve Closing (EIVC). The three operating states in mDSF can be used to simultaneously optimize engine efficiency and driveline vibrations. Acceleration performance is retained using the all-cylinder, high-charge firing mode.

Although mDSF can be implemented with a variety of valvetrains, the most cost-efficient solution for mDSF is comprised of asymmetric intake valve lifts and/or ports, with one high-flow power charging port and one high-efficiency Miller port. The power charging port is deactivated

independently, whereas the Miller port deactivation is coupled to the exhaust valves. High-charge firing is realized with all four valves active, low-charge firing is realized with the power valve deactivated, and skip is realized with all four valves deactivated.

The mDSF asymmetric valve strategy was compared to the baseline symmetric valve strategy through dynamometer tests in a production Miller cycle engine and minimal degradation in efficiency was observed. Maximum torque was reduced by 3-8% for mDSF, but it is expected that this can be recovered with combustion system optimization. Engine fuel consumption maps were generated based on experimental data and mDSF "flyzones" were estimated using Tula's extensive noise, vibration and harshness (NVH) database and experience. Compared with a production state-of-the-art Miller cycle engine baseline, mDSF was projected to reduce fuel consumption by 9.5% in the US City-Highway cycle and 7.5% in the WLTC (Class 3). Combined with a relatively low added cost of the proposed valvetrain design, mDSF presents an unparalleled cost-benefit ratio in the market with relatively short-term production viability.

Introduction

The transportation sector consumes a significant portion of all energy produced globally, mostly as fossil fuels such as gasoline and diesel, which release greenhouse gases and other potentially harmful emissions when converted into mechanical work. The internal combustion (IC) engine has improved steadily since its inception, but the challenges ahead posed by government regulations, climate change and increasing demand are global in scale and will not be easily met. The highly competitive automotive space has also led to more demanding customers unwilling to accept compromises in acceleration performance, fuel efficiency and comfort. Due to high cost and slow adoption of electrified powertrains, the industry estimates a billion IC engines will be on the road by 2045 [1], so they must continue to improve at an accelerated pace. Emerging technologies such as Dynamic Skip Fire (DSF) [2, 3, 4, 5, 6, 7] and well-understood strategies like the Miller cycle [8, 9, 10, 11, 12, 13] are starting to see production applications by offering attractive

fuel economy gains without costly aftertreatment systems associated with lean combustion engines.

Tula has developed a novel concept designated as mDSF, which integrates Dynamic Skip Fire and Miller cycle engines. At a given engine state, mDSF improves torque waveform control by employing three cylinder states, i.e., two firing levels and deactivation. mDSF delivers additive and synergistic fuel efficiency benefits by addressing the limitations that individually affect the underlying DSF and Miller cycle technologies, while only requiring a modest increase cost from added hardware.

The objective of this report is to present engine test results and vehicle fuel efficiency projections demonstrating the fuel consumption improvements made possible with mDSF. DSF and Miller cycle are first described as a foundation to the mDSF cylinder deactivation technology. mDSF is then presented in detail, with discussion of sources for improved efficiency and improved noise, vibration and harshness

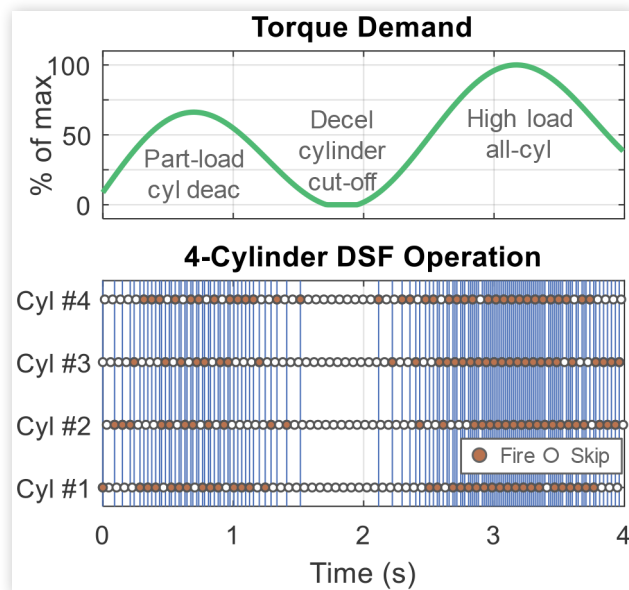
(NVH). The mechanical implementation and controls considerations are also discussed. These results are contrasted with all-cylinder engine test results. In-depth model-based analysis is used to interpret test results and expand understanding of charge motion trends. Finally, vehicle drive cycle simulations are used to estimate the potential improvement of mDSF relative to a state-of-the-art production 2-step Miller cycle engine.

Dynamic Skip Fire

Dynamic Skip Fire (DSF[®]) is a proven cylinder deactivation technology for throttled IC engines that can deliver significant fuel economy improvements via reduction of pumping losses in part-load operation. In part-load DSF operation, proprietary control algorithms are used to dynamically fire or skip individual cylinders on a cycle-by-cycle basis. Torque is delivered at optimum efficiency through a continuously evolving firing frequency that also satisfies rigorous NVH targets required by automotive manufacturers [2, 3]. The engine returns to normal all-cylinder operation at high torque demands, so there is no negative impact to acceleration performance. A conceptual cylinder history is shown in Figure 1. The DSF technology is primarily centered on software and can be implemented in all valvetrain architectures capable of intake and exhaust valve deactivation.

DSF also improves combustion stability, enhances transient torque control, and enables Deceleration Cylinder Cut-Off (DCCO) where all of the cylinders are deactivated

FIGURE 1 Conceptual firing history of DSF engine for transient torque demand. At lower torques, DSF dynamically deactivates cylinders on a cycle-by-cycle basis to maximize efficiency with production-level NVH. Engine switches to all-cylinder operation when torque demand is high. DSF also enables Decel Cylinder Cut-Off, where all cylinders are deactivated, when torque demand is zero.



© 2019 SAE International. All Rights Reserved.

(fuel disabled and valves closed), as shown in Figure 1. During DCCO, no air is pumped through the engine as in conventional Deceleration Fuel Cut-Off (DFCO) where only fuel is disabled, thereby reducing engine braking, prolonging fuel cut-off time and minimizing catalyst refuel penalties. Further fuel economy gains can be achieved with passive or pre-tuned NVH mitigation hardware, as well as torque converter clutch slip in automatic transmissions.

DSF has been demonstrated with great success in V8 engines, achieving drive cycle fuel efficiency gains of 14% to 18% in a 2010 GMC Yukon Denali with NVH indistinguishable from the baseline production vehicle [2, 4]. General Motors has now rolled out the technology under the name Dynamic Fuel Management into two production V8 applications [5]. For vehicles with downsized-boosted 4-cylinder engines, DSF can also deliver significant fuel consumption improvements of 6% to 8% [6, 7]. The relatively low cost of cylinder deactivation hardware further improves the production value of DSF.

Despite the positive outlook, the potential for DSF is more limited in smaller engines with reduced cylinder count due to overall lower firing frequencies, coarser firing density resolution and higher engine loads, which deteriorate NVH. Tula has developed solutions for next generation DSF-centered technologies that align with industry trends by integrating powertrain electrification (eDSF) [14], Miller cycle engines (mDSF), lean gasoline engines (λ DSF) [15], diesel engines (dDSF) [16], and autonomous vehicles (aDSF) [17].

Miller Cycle Engines

Miller cycle engines are also gaining traction in the industry as the downsized-boosted engine trend faces growing challenges with real world fuel economy and emissions. Although Miller originally developed an engine with an auxiliary compression control valve [8], in today's automotive industry jargon, the Miller cycle is an over-expanded thermodynamic cycle where the expansion ratio is larger than the compression ratio, achieved through early intake valve closing (EIVC) or late intake valve closing (LIVC). Implemented with some level of intake air supercharging (or turbocharging) and increased cylinder displacement, a Miller cycle can extract additional work from a given amount air-fuel charge, thereby increasing the thermal efficiency [9, 10, 11, 12]. The Atkinson cycle is another example of an over-expanded thermodynamic cycle and is sometimes used interchangeably with the Miller cycle.

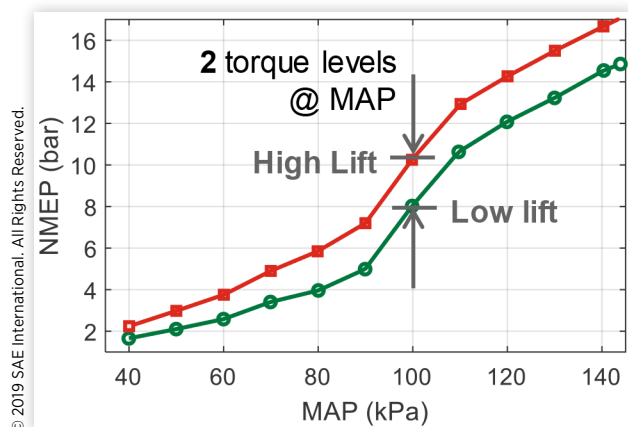
Miller cycle engines can deliver benefits throughout the usable operating range and has made it into several production applications. As demonstrated by the new EA888 2.0L Gen. 3B [13] from the Audi/VW group, a production Miller cycle that delivers substantial reductions in fuel consumption compared with the previous generation EA888 1.8L Gen. 3. Published engine maps with brake specific fuel consumption (BSFC) show improvements on the order of 5% to 15% depending on engine speed and load, which translates into 3% to 6% lower vehicle CO₂ emissions. This includes friction improvements enabled by lower specific loads in the upsized engine.

The EIVC strategy employed in Miller cycle engines has significant impacts on in-cylinder charge motion and subsequent combustion behavior. Specifically, by shortening the intake stroke with EIVC there is less time to introduce flow energy and more time for turbulence to decay before the ignition event. These will be detrimental to flame propagation, resulting in longer burns and worse combustion stability. Therefore, special attention must be paid to the design of the combustion system to maintain combustion quality and achieve maximum efficiency. This will typically require steeper intake port angles, valve masking and piston crown shaping to enhance tumble motion during the shorter intake and conserve it through the spark ignition event [13].

Implementation of a Miller cycle strategy also means airflow will be more restricted given the lower lift, shorter duration intake valve events. Higher intake air pressures are therefore required to satisfy engine performance targets. This typically leads to a compromise between maximum power and best efficiency. A 2-step intake valve lift system can alleviate this compromise by offering a more optimal low power aggressive Miller cycle configuration to maximize part load efficiency and a high power configuration with increased airflow capacity to deliver peak torque. In current production applications, however, the low lift Miller cycle follows a relatively mild design, so it can have enough torque capacity for most normal driving conditions. This compromised design minimizes the fuel consumption penalty of mode transitions but limits the potential efficiency benefit of the Miller cycle engine.

Figure 2 describes several key traits of 2-step Miller cycle engines based on experimental results from the EA888 Gen. 3B engine on Tula's engine dynamometer. The top panel demonstrates the different torque output levels in terms of net mean effective pressure (NMEP) of the two valve lift configurations at 1500 rpm, where Low Lift indicates the Miller cycle mode and High Lift indicates the high power mode. NMEP for the Low Lift is approximately 80% of the High Lift at 100 kPa MAP. This ratio can vary with speed and load due to relative differences in pumping friction.

FIGURE 2 Torque output characteristics of production 2-step Miller cycle engine (Audi EA888 Gen. 3B) for low lift and high lift modes at the same nominal operating conditions. The low lift delivers 20% less torque at 100 kPa MAP.



© 2019 SAE International. All Rights Reserved.

FIGURE 3 BSFC comparison between of the Miller cycle engine and its previous generation non-Miller counterpart. The low lift mode of the Miller cycle engine reduces fuel consumption by 12% at 3 bar BMEP.

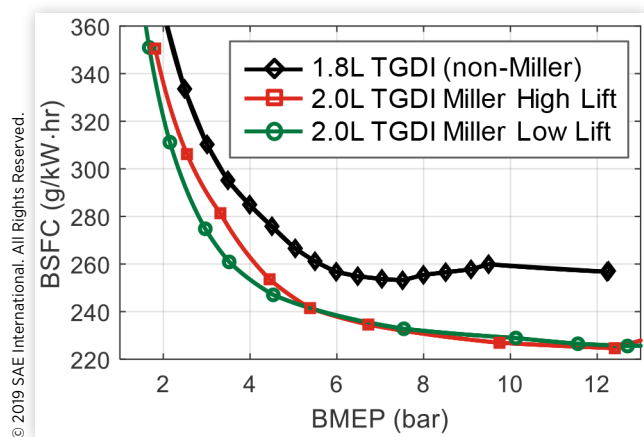
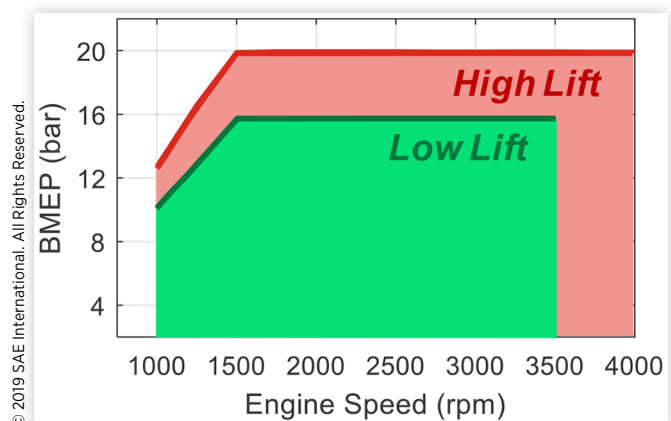


Figure 3 compares the fuel consumption of the two Miller cycle engine modes with the previous generation 1.8L non-Miller engine. At 3 bar, the Low Lift reduced fuel consumption by 12% and the High Lift by 6.5%. Note, the two engines did not use the same fuels, so part of the difference may be attributed to fuel heating value and stoichiometric air-fuel ratio. Comparing the two Miller cycle engine modes, the Low Lift configuration delivers more than 5% better fuel consumption than the High Lift below 6 bar. Even though no improvement is observed above this load, similar fuel consumption is maintained. This allows the Low Lift operating range to be extended, which will minimize costly mode transitions and improve vehicle fuel consumption. This is more clearly illustrated in Figure 4 showing the speed and load operating ranges for the Low Lift and High Lift modes of the Miller cycle engine up to 4000 rpm. The Low Lift configuration is capable of 16 bar BMEP and can operate up to 3500 rpm. This should cover the majority driving conditions in certification drive cycles and real-world settings. The valvetrain dynamics resulting from

FIGURE 4 Maximum torque output for the Miller low lift and high lift. The low lift configuration was designed to expand the high load operating range and cover most normal driving conditions.



© 2019 SAE International. All Rights Reserved.

more aggressive Miller cycle valve lifts may limit Low Lift operation at higher engine speeds.

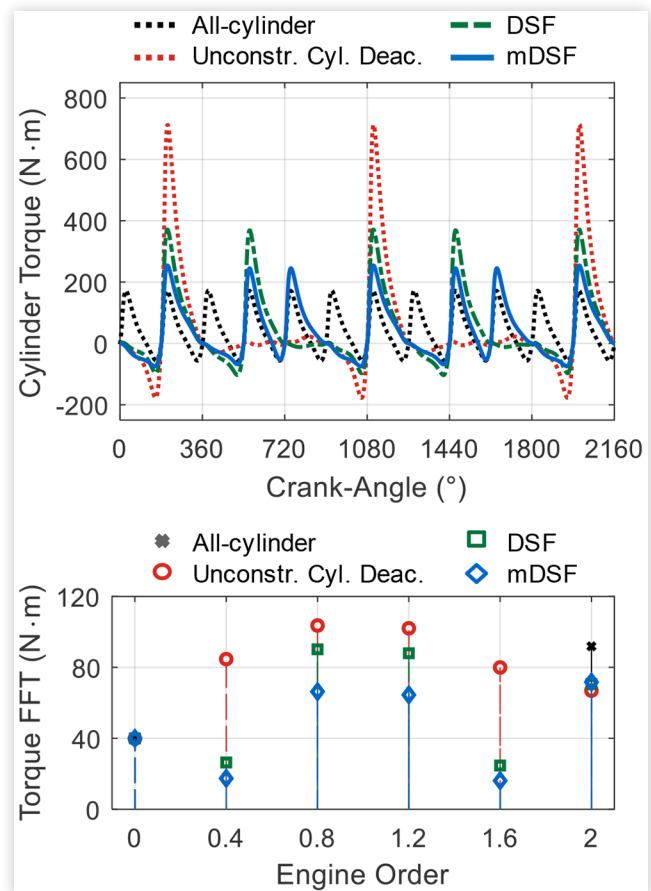
mDSF Cylinder Deactivation Technology

The mDSF concept intelligently combines powerful DSF and Miller cycle engine technologies to deliver additive and synergistic fuel efficiency benefits by simultaneously addressing the NVH constraints and efficiency-power tradeoffs that limit these individual technologies. mDSF takes advantage of the multi-level charge and torque characteristic of 2-step Miller cycle engines shown in [Figure 2](#), such that individual cylinders can dynamically switch among three operating states: high charge firing or Hi Fire (high cylinder load), low charge firing or Lo Fire (low cylinder load, achieved through aggressive Miller cycle), and deactivation or skip. These are selected on a cycle-by-cycle basis to deliver the requested engine torque at high efficiency and provide enhanced control over the engine torque waveform, which can be used to more effectively mitigate NVH issues. Ultimately, mDSF aims to deliver minimum fuel consumption and satisfactory acceleration performance at minimal added cost compared with DSF and Miller cycle.

[Figure 5](#) illustrates the potential benefits of mDSF using a simple torque waveform simulator based on measured cylinder pressure data. The top panel shows four waveforms producing a mean engine torque of 40 N·m at 1500 rpm on a 4-cylinder engine. All-cylinder operation displays the lowest amplitude torque pulses and highest firing frequency. The engine is heavily throttled with a manifold pressure (MAP) of 35 kPa. Fast Fourier Transform (FFT) analysis of the torsional vibration (bottom panel) indicates a high 2nd order component, lower orders are negligible. Unconstrained cylinder deactivation operating at the lowest possible firing density to achieve maximum efficiency displays the lowest frequency and highest amplitude torque waveform. This would result in completely unacceptable NVH, as can be appreciated by the high amplitude low order components of the FFT. Tula's DSF manages these undesired excitations to maintain production-quality NVH by selecting the most efficient but NVH-acceptable firing density to deliver engine torque. Compared with the all-cylinder case, MAP increases significantly to 68 kPa, thus cutting pumping losses by nearly half. The FFT shows DSF reduces the 0.4 and 0.8 order vibration components by 69% and 13%, respectively, relative to the unconstrained case. mDSF further improves upon DSF in terms of NVH by introducing an additional firing event and operating in low charge Miller mode, such that the efficiency penalty is minimal. MAP decreased by only 2.6 kPa, while the amplitude of the 0.8 and 1.2 orders were reduced by 26.7%. mDSF also allows special firing sequences that alternate firing events between high charge and low charge modes, which could offer additional opportunities for NVH improvement.

[Figure 6](#) shows a conceptual mDSF firing history for a 4-cylinder engine (bottom panel) as a function of driver torque demand relative to maximum engine torque (top panel).

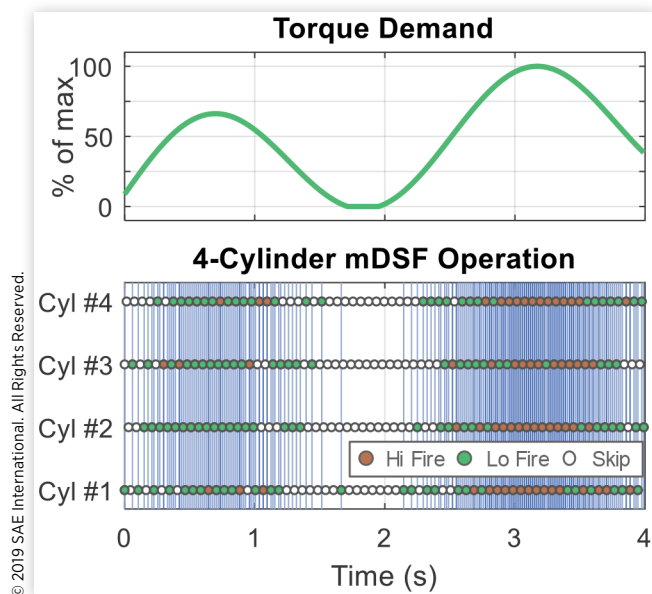
FIGURE 5 Conceptual NVH benefit of mDSF. Top panel shows torque waveforms for all cylinder operation, unconstrained cylinder deactivation, DSF and mDSF. The bottom panel shows the FFT of the torque waveform, indicating amplitude of torsional vibration modes. Unconstrained cylinder deactivation with very low firing density produces unacceptable NVH, whereas DSF and mDSF deliver production-viable NVH by adequately managing firing sequences. mDSF allows for higher firing densities for further improved NVH without an efficiency penalty.



Note the use of three cylinder states designated as Hi Fire, Lo Fire and Skip. Compared with DSF ([Figure 1](#)), mDSF would result in 35% more firing events for the same torque demand trace. mDSF retains all the key benefits introduced by standard DSF including DCCO and delivers the expected acceleration performance by switching to all-cylinder, Hi Fire mode at high torque demands. Furthermore, mDSF enables the use of more aggressive Miller cycle designs that have better low load efficiency but reduced load range by employing advanced DSF-based algorithms that enable smoother and more efficient transitions between low and high charge modes. This effectively eliminates the efficiency-power tradeoff faced by current Miller cycle engines.

The efficiency and NVH improvement potential of mDSF is highly dependent on the 2-step Miller cycle engine design. The ratio of torque between the low and high charge modes at a given manifold pressure (and other global engine parameters such as cam phasing) determines the vibration

FIGURE 6 Conceptual firing history of mDSF engine for transient torque demand. At lower torques, mDSF operates mainly in Lo Fire and Skip modes, and switches to all-cylinder Hi Fire when torque demand is high. Note the dynamic transition between Lo Fire and Hi Fire.



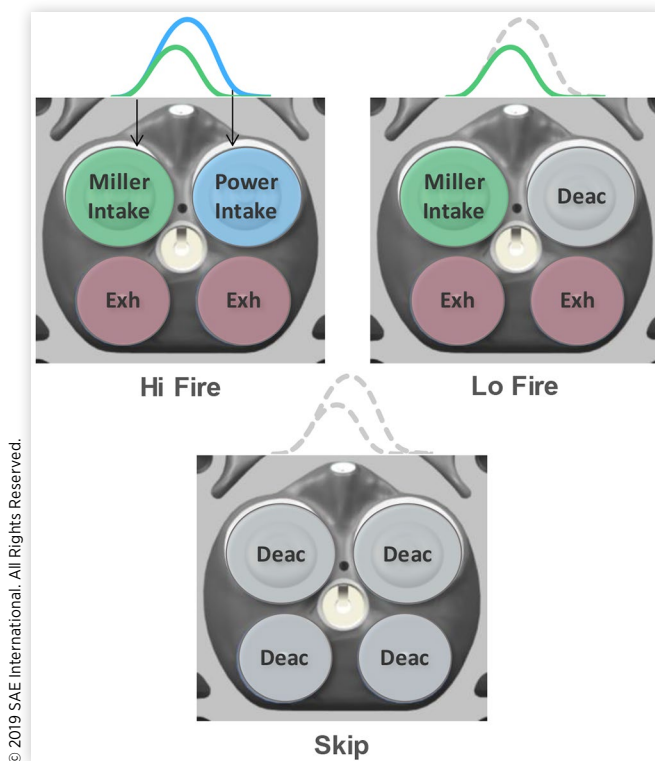
characteristics and load range of viable firing densities. This ratio typically ranges from 0.6 to 0.8, where lower values will generally indicate a more aggressive Miller cycle strategy for the low charge mode. A holistic approach should be used to optimize this ratio together with the mDSF strategy for maximum efficiency benefit.

Valvetrain Hardware and Combustion System

Valvetrains with more than two valve lift stages as required by mDSF are uncommon in production due to cost and packaging challenges. Fully-variable lift systems are available, but production implementations usually lack the ability to control cylinders individually [18, 19]. Valvetrains with sliding cam elements are also capable of 3 stages [20] but are currently constrained in terms of cycle-to-cycle and individual cylinder mode switches. mDSF, however, does not require a completely new and costly 3-step valvetrain mechanism.

The most cost effective valvetrain configuration proposed for mDSF can employ an existing valve deactivation mechanism currently used for DSF, combined with asymmetric intake valve lifts/ports and independent deactivation control of the two intake valves in each cylinder. This mechanization strategy for mDSF is illustrated in Figure 7. The Hi Fire mode is achieved with all valves active and delivers the highest cylinder torque. Notice the use of two distinct intake valve lifts (or ports): the Miller Intake and the Power Intake. The Miller Intake valve has a lower lift, shorter duration with EIVC as would be found in the lower stage of a 2-step Miller cycle engine. The Power Intake has a higher lift, longer duration valve lift to maximize airflow and torque. Even though the

FIGURE 7 Proposed cost-effective valve strategy to achieve three cylinder modes in mDSF. Requires asymmetric valve lifts and independent deactivation of one intake valve. This can be achieved with production-ready valve deactivation hardware.

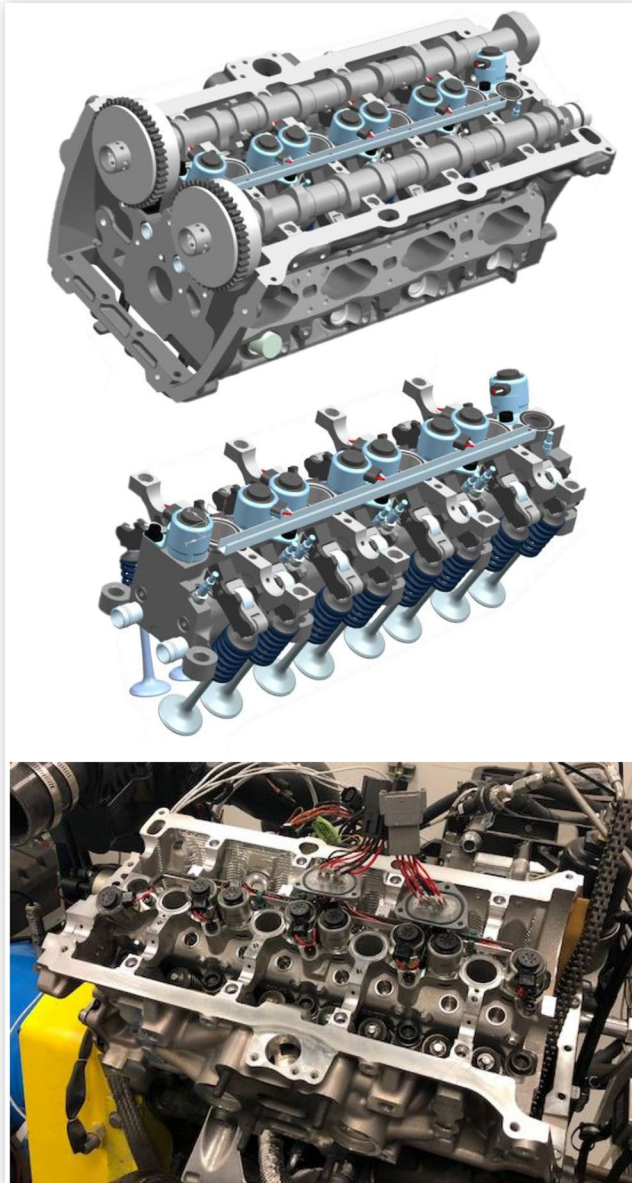


Miller Intake valve is used in the Hi Fire mode, the Power Intake primarily controls cylinder charge and effective compression ratio. In the Lo Fire mode, the Power Intake valve is deactivated, resulting in a lower cylinder charge and true Miller cycle operation. Finally, the Miller intake is deactivated together with the exhaust valves to realize the Skip mode or full cylinder deactivation.

Depending on the valvetrain type, this strategy could be implemented mechanically using production-ready deactivatable roller finger followers (dRFF) or deactivatable lifters [21]. In a hydraulically controlled system, two (2) oil control valves (OCV) would be required for each cylinder. One OCV controls the activation state of the Power Intake valve and another OCV controls the activation state of the Miller Intake and Exhaust valves. Electronically controller dRFF's are also in development and would ideally suited for mDSF due to reduced design complexity of the oil control manifold and associated packaging challenges.

In most engines in production, the asymmetric intake valve lifts/ports would impact combustion due to disturbances in charge motion and reduction in overall flow areas. This may be an important concern to an OEM and presents one of the primary risks associated with the mDSF technology. Single port operation, however, has been shown to offer benefits in efficiency and emissions control [22, 23]. The results of Tula's internal investigation on this topic are also discussed in the Engine Testing section below. Reference [23] further

FIGURE 8 Prototype mDSF cylinder head developed in partnership with FEV. Top and mid panels show CAD models of the valvetrain, including deactivatable roller finger followers (dRFF) on each valve, two oil control valves (OCV) per cylinder, an oil distribution manifold and custom camshafts. Design was integrated into modified production cylinder head for EA888 Gen. 3B engine. Bottom panel shows partially assembled cylinder head installed on Tula's engine dynamometer. Engine is now operational and undergoing extensive testing.



demonstrates the possibility of an optimized asymmetric port design, where one of the intake ports maximizes tumble motion and reduces swirl motion in single port operation, and the second port acts as a charge port. This design delivers maximum airflow and power in dual port operation. Unconventional port geometry and valve masking played key roles to achieve the air flow and charge motion targets. This level of combustion system optimization for mDSF would

ensure best engine performance from the standpoint of fuel efficiency, emissions and acceleration.

In 2018, Tula Technology partnered with FEV North America to design and build a series of fully functional prototype cylinder heads. The mDSF valvetrain consisted of prototype dRFF's, OCV's and HLA's units currently used in DSF demonstration programs [21], built into modified cylinder heads from an Audi/VW EA888 Gen. 3B 2.0L, 4-cylinder engine [13]. A new hydraulic manifold was designed to accommodate eight (8) OCV's and manufactured using Selective Laser Melting (SLM). Custom camshafts were created from billet, with stock cam phasers welded onto the ends using stock TDC alignments. Figure 8 shows a set of CAD models of the mDSF cylinder head, as well as a picture of the actual hardware installed on the engine at Tula's engine dynamometer. Details of the design and manufacturing process can be found on a separate publication [24]. Test results from the mDSF prototype engine will be published in 2019.

Control Strategies and Algorithms

DSF implementation affects many control structures in the engine torque control path. In addition to the cylinder deactivation and firing control block, air management, fueling and ignition, among others, also need to be considered. mDSF extends the controls requirements of DSF with a second firing mode and a third valvetrain mode. The two firing modes call for additional calibrations and a proper accounting of Miller cycle sensitivities such as intake cam phasing and effective compression ratio. Accurate cycle-by-cycle in-cylinder air estimation models for each charge level are important to achieve best efficiency and drivability.

The fuel consumption benefit of DSF and mDSF technologies also depends strongly on the advanced digital signal processing (DSP) algorithms used to dynamically control firing sequences to maximize efficiency and minimize engine vibrations. Although the details of these are beyond of the scope of this paper, several important concepts concerning mDSF are worth defining.

In standard DSF, the notion of Firing Density (FD) is commonly used to indicate the proportion of *firing* events out of a given *total* amount of cylinder events including deactivation or skips. A $FD = 0.5$ means that 1 out of every 2 possible events is fired. This is equivalent to 2-cylinder operation in a 4-cylinder engine or 4-cylinder operation in an 8-cylinder engine. In mDSF, there are two possible firing modes, previously designated as Hi Fire and Lo Fire, that induct different air charges and produce different torque pulses. C is therefore defined as the low-to-high charge ratio at a nominal operating condition and ranges from 0 to 1. C is a key engine design parameter for mDSF. To track the firing states, a new parameter HS is defined, which indicates the share of *Hi Fire* events out of the total *firing* events. A conventional Miller cycle would therefore operate at either $HS = 0$ or $HS = 1$. mDSF, however, allows for $0 \leq HS \leq 1$. Finally, with mDSF it is also possible to generate hybrid sequences of Hi Fires, Lo Fires and Skips, resulting in an *effective* FD defined as:

$$eFD = FD \cdot [HS + (1 - HS) \cdot C] \quad (1)$$

The eFD concept is mainly useful when comparing to FD's in standard DSF and relating these to engine torque output. FD, HS and C are more relevant for actual engine controls and are used to schedule firing sequences consistent with Tula's proprietary algorithms [25].

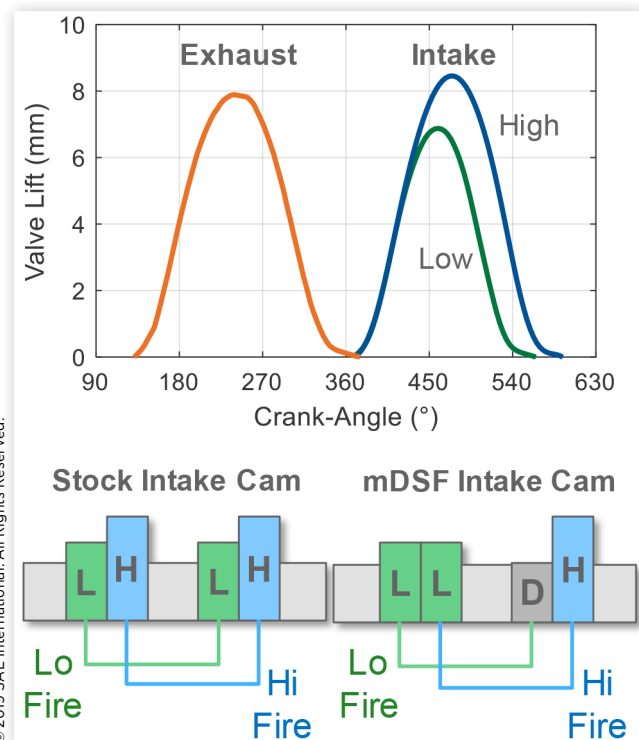
Engine Testing

The initial phase of mDSF engine testing had two main objectives: 1) understand all-cylinder engine operation with asymmetric cams and 2) deliver steady-state engine fuel consumption maps to project mDSF vehicle drive cycle fuel consumption improvements. The following sections describe the experimental setup, test results and detailed combustion analysis of the base mDSF engine operating in all-cylinder mode, which will later become the foundation for true mDSF operation.

Experimental Setup

The benefit of mDSF relies in part on the efficiency of the underlying Miller cycle engine, so an optimized Miller cycle combustion system with adequate combustion quality and efficiency is highly desired. The new Audi 2.0L EA888 Gen. 3B, a state-of-the-art 4-cylinder, turbocharged, direct-injected, 2-step Miller cycle engine [13] was therefore chosen as the mDSF development platform. Engine specifications are shown in Table 1. The 2-step sliding cam valve lift system provided the capability to easily switch between low lift (Lo Fire) and high lift (Hi Fire). The measured valve lift curves at minimum overlap are shown in Figure 9. At maximum intake cam advance, the low lift Miller cam closes approximately 60°CA before BDC. The high lift cam results in a milder Miller cycle and is desired not only for the inherent efficiency benefits, but also as a way to manage the effective compression ratio at high loads. A custom camshaft was also created to realize the mDSF

FIGURE 9 Top panel: Intake and exhaust valve lifts for the EA888 Gen. 3B engine at parked phaser positions (maximum exhaust advance and intake retard). Bottom panel: Sliding cam elements for stock and mDSF configurations. Notice the modified cam lobes on the mDSF cam to realize asymmetric lift strategy.



© 2019 SAE International. All Rights Reserved.

asymmetric valve lift / port configurations as shown in Figure 9. The stock low lift and high lift cam lobes were retained. Full cylinder deactivation was not possible with this valvetrain hardware. Test fuel with an average octane number of 93 was used based on the OEM specification for the stock engine.

Stock engine calibrations were reverse engineered from a 2017 Audi A4 Ultra through steady state testing on an eddy current chassis dynamometer. Engine controls were then implemented in a dSPACE rapid prototyping hardware consisting of a MicroAutoBox and a 4-layer RapidPro stack with sufficient I/O channels and adequate drivers to operate the engine similar to the stock engine control unit (ECU). The basic control software architecture was derived from Tula's previous experience with Audi/VW engines, extended and improved where necessary for the new EA888 Gen. 3B engine. The dSPACE 2014-A RTI blockset was used with MATLAB/Simulink 2014a to build the embedded code.

The engine was installed on a SuperFlow eddy current engine dynamometer and operated using WinDyn data acquisition system. Brake torque was measured with an Interface model SSM Sealed S-Type Load Cell achieving 0.02% nonrepeatability. In addition to OEM sensors for mass air flow (MAF), manifold absolute pressure (MAP), intake air temperature (IAT), charge pressure and temperature, engine instrumentation included low-speed Omega absolute pressure sensors and K-type thermocouples throughout the

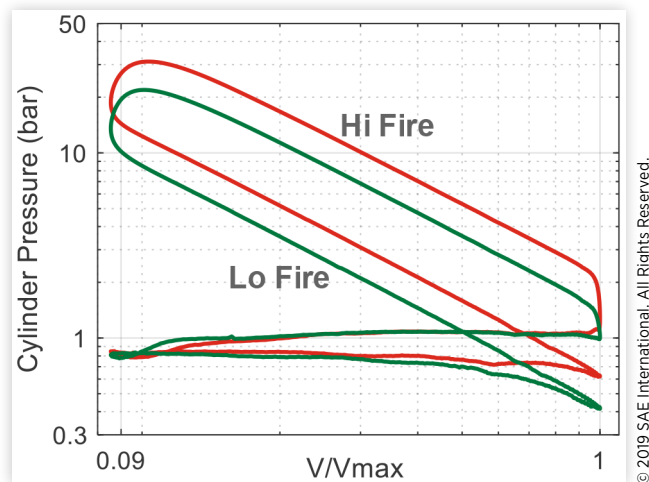
TABLE 1 Engine specifications for Audi EA888 Gen. 3B.

Engine configuration	4-cylinder, inline, TGDI
Displaced volume	1984 cm ³
Bore x stroke	82.5 mm x 92.8 mm
Compression ratio	11.7:1
Maximum Torque	320 N-m @ 1450-4200 rpm
Maximum Power	142 kW @ 4200-6000 rpm
Valve lift control	2-step sliding cam elements
Low lift valve profile	Duration @ 1 mm: 140°CA Max lift: 6.9 mm
High lift valve profile	Duration @ 1 mm: 170°CA Max lift: 8.5 mm
Cam phaser authority	Intake: 0 to 60°CA advance Exhaust: 0 to 30°CA retard
Intake ports	Tumble enhanced design w/valve masking and tumble flaps
Combustion chamber	Tumble conserving piston and pent-roof
Test fuel	Gasoline 93 ON

© 2019 SAE International. All Rights Reserved.

© 2019 SAE International. All Rights Reserved.

FIGURE 10 Measured pressure-volume diagram on a log-log scale for Low lift and High Lift Miller cycle configurations at 1500 rpm, 80 kPa MAP, 60°C intake cam advance and 10°C exhaust cam retard. The Low Lift mode shows earlier intake valve closing and a lower effective compression ratio.



air handling system. A Micro Motion® ELITE® Coriolis Flow meter with a $\pm 0.10\%$ nominal accuracy was used to measure fuel mass flow rate upstream of the high-pressure DI pump. An ECM Lambda sensor was installed after the turbine for closed-loop air-fuel ratio control. AVL GH13Z-31 spark-plug style high speed in-cylinder pressure transducers with a range of 0-150 bar and a linearity of 0.10% of full-scale output were sampled using an encoder with 0.5°CA resolution on A&D CAS 5.3. The TDC measurement had a standard deviation of 0.69°CA. In-cylinder pressure was pegged using a polytropic method assuming a polytropic exponent of 1.3. Control signals were also logged in dSPACE ControlDesk 5.2 with a base sampling rate of 10 kHz. O₂, CO, CO₂, THC and NO_x emissions were measured using a Horiba MEXA-One unit through a heated sampling line downstream of the turbine.

Figure 10 shows a pair of sample pressure-volume diagrams for low lift and high lift modes at the same nominal engine speed, manifold pressure and cam phasing. The low lift pressure trace clearly illustrates the Miller cycle characteristics, where EIVC lowers the compression line and effectively reduces the compression ratio compared with the expansion ratio. The high lift pressure trace exhibits similar characteristics, but at a reduced scale. For these operating conditions, the ratio in NMEP between the low lift and high lift modes is 67%.

Fuel Consumption Results

Engine testing and calibration primarily focused on all-cylinder operation comparing the stock valve lift configuration (symmetric low and high lift) to the mDSF asymmetric low and high charge configurations. The goal was to understand the impact on fuel consumption and torque output, which could then be used to establish a path for improvements of mDSF technology.

Steady state part-load engine tests were carried out at four engine speeds: 1250, 1500, 2000 and 3000 rpm. MAP was swept from 40 kPa to 180 kPa (or maximum for each engine speed) in 10 kPa intervals. For the stock configuration, the reverse engineered calibrations for intake cam phasing, exhaust cam phasing, fuel rail pressure and injection timing were used directly. Minor adjustments in spark ignition timing were made to maintain desired combustion phasing (CA50) ranging from 4°CA at low loads to 8°CA and later at moderate to high loads. COV of IMEP was maintained below 2.5%. For the mDSF asymmetric configurations, intake and exhaust cam phasing was optimized for best fuel consumption, while assuming the same combustion phasing and stability targets. The key results from these tests are summarized in Figure 11 through Figure 15.

Figure 11 shows the net specific fuel consumption (NSFC) as a function net indicated mean effective pressure (NMEP) at the four tested engine speeds for the stock symmetric low lift configuration (two intake valves in low lift mode) and the mDSF asymmetric low charge configuration (one intake valve in low lift mode and another intake valve deactivated). The two configurations show similar fuel consumption through most of the speed and load range. Lower tested boundaries were associated with increasing combustion instability, whereas the upper tested boundaries were generally associated with knock. At 3000 rpm, the mDSF asymmetric low charge mode was limited by airflow through the single port and exhibited overall worse fuel consumption due to increased flow friction and pumping work.

Figure 12 shows several key calibration parameters at 1500 rpm used to achieve the fuel consumption results in Figure 11, with associated combustion and emissions results in Figure 13 and Figure 14, respectively. Overall, most of the trends are similar between both configurations. In both cases, intake cam is most advanced in the 2-5 bar NMEP range. At lower loads, the intake cam must be retarded to manage the residual gas fraction and maintain combustion stability, which rapidly decreases below 4 bar NMEP. At higher loads, the intake cam is also retarded to allow more airflow and increase the effective compression ratio. Spark timing is also most advanced at low loads where the charge is highly diluted and becomes retarded at higher loads to mitigate knock as indicated by the retarded CA50.

For the mDSF 1-valve configuration, however, MAP is approximately 10 kPa higher on average throughout the load range, which results from the more advanced intake cam phase and reduced flow area for the same nominal cylinder air charge. Spark timing was advanced in order to achieve equivalent combustion phasing (CA50) targets. This is may be required in part to compensate for the charge motion differences, i.e. tumble and swirl, between 1-valve and 2-valve configurations. This could also partially explain the slightly longer 10-90% burn durations. The exhaust cam phasing trend is significantly different, but this can be attributed to the optimization approach. Exhaust cam phasing generally did not produce large efficiency changes, so a calibration similar to stock would likely show similar results. Emissions were also comparable, although CO and THC seemed to improve with the mDSF 1-valve configuration at higher loads, whereas NO_x was slightly higher. It's possible in-cylinder

FIGURE 11 Comparison of NSFC between low charge (Lo Fire) stock symmetric intake valve lifts and mDSF asymmetric intake valve lifts as a function of load for various engine speeds. The mDSF asymmetric low charge strategy shows very similar fuel consumption trends compared with the stock symmetric strategy. This indicates mDSF would not need to overcome an efficiency loss and can instead deliver additive or synergistic improvements from the base Miller cycle engine through cylinder deactivation.

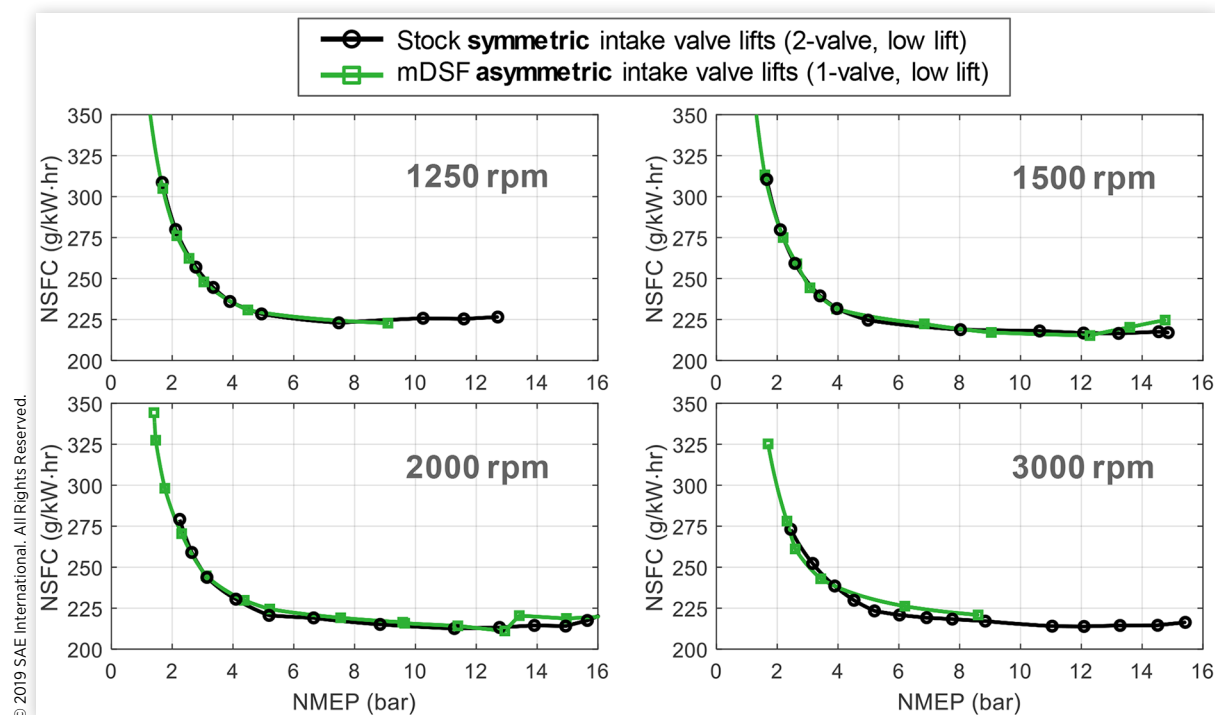


FIGURE 12 Comparison of optimum engine calibration between low charge (Lo Fire) symmetric and asymmetric intake valve lifts for key parameters at 1500 rpm. General trends are similar, with some notable differences. The mDSF asymmetric operates with a more advanced intake cam phase and higher manifold pressure. Spark advance is also earlier, likely to account for changes in charge motion and turbulence near TDC. The exhaust calibration is provided minimal improvements in combustion stability and could easily be smoothed out to facilitate transient controls.

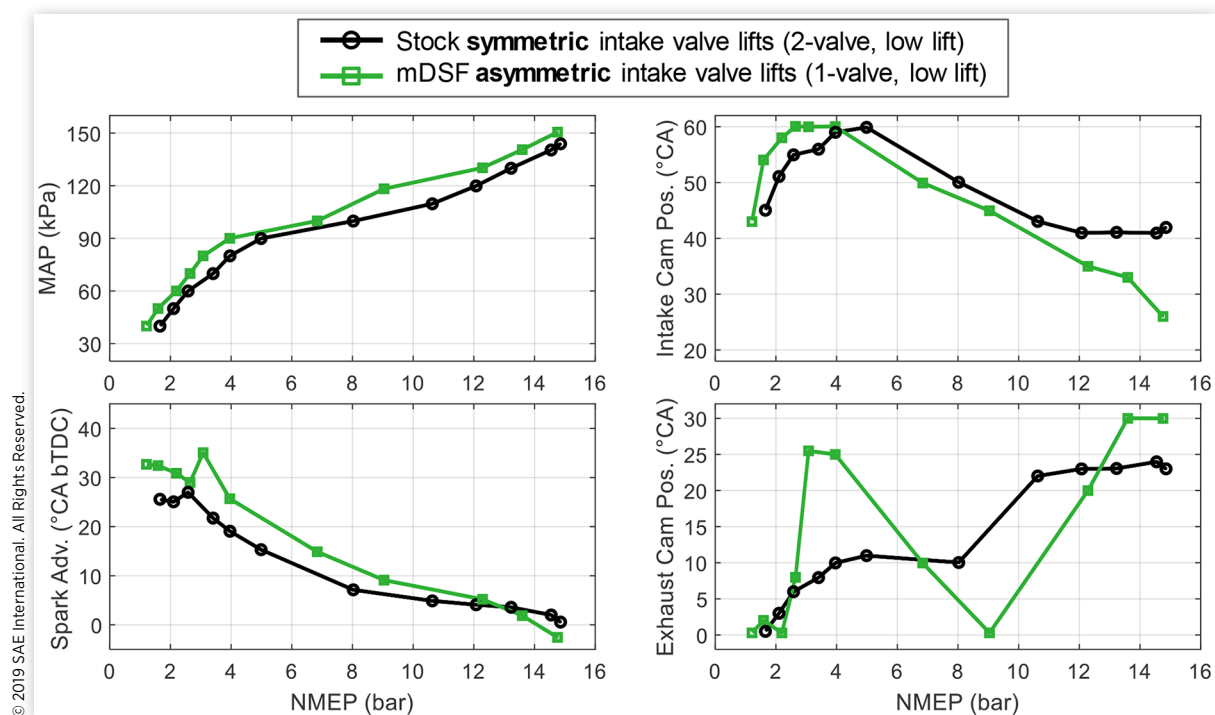
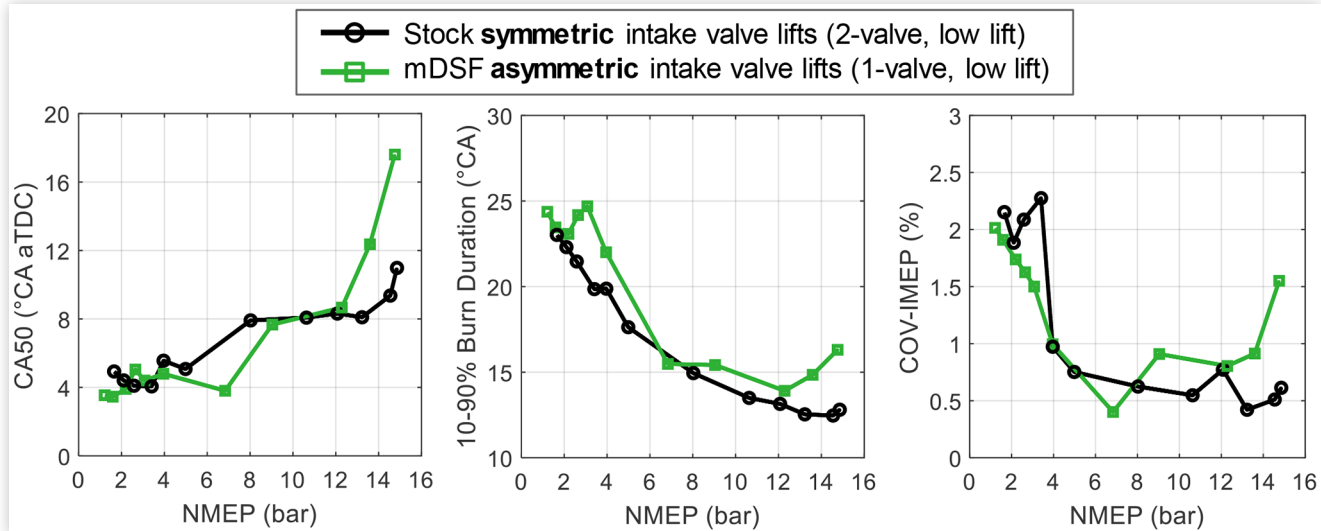
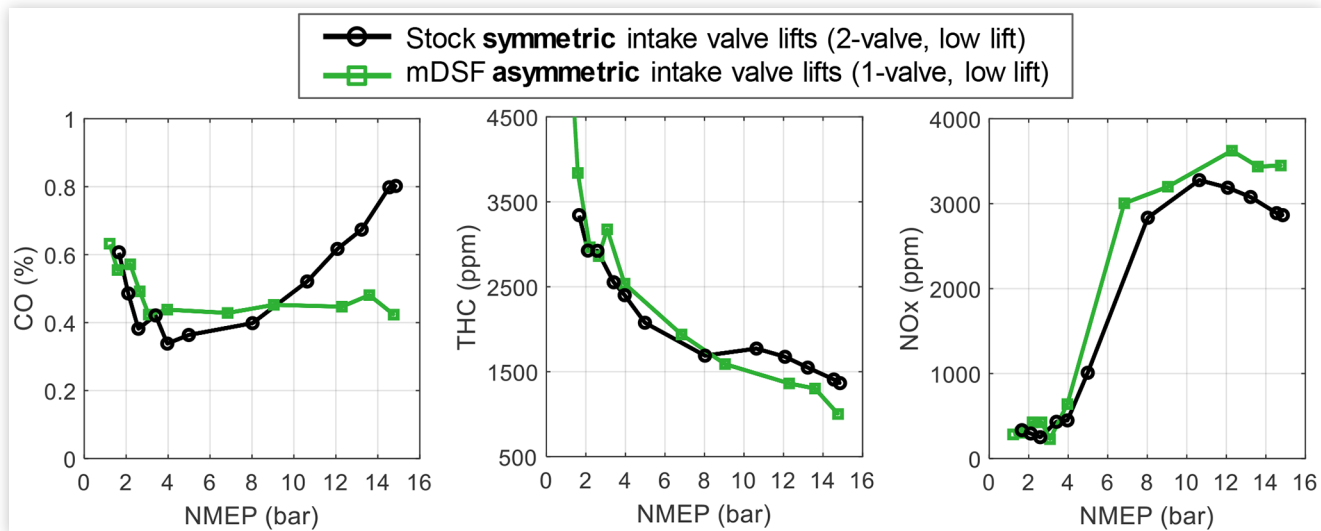


FIGURE 13 Comparison of combustion performance between low charge (Lo Fire) symmetric and asymmetric intake valve lifts at 1500 rpm. Both configurations exhibited similar combustion characteristics through moderate loads. The mDSF asymmetric configuration burned slightly slower and at higher loads was more retarded and unstable. This not a concern since in vehicle operation a switch to Hi Fire mode would have been enforced.



© 2019 SAE International. All Rights Reserved.

FIGURE 14 Comparison of engine emissions between low charge stock symmetric and mDSF asymmetric intake valve lifts at 1500 rpm. Results were similar at lower loads, but at high loads the mDSF asymmetric strategy reduced CO and THC while increasing NO_x. This trend may be due in part to higher in-cylinder temperatures from longer burn durations, which would promote oxidation but also accelerate NO_x production.



© 2019 SAE International. All Rights Reserved.

temperatures were hotter, helping oxidation but increasing NO_x production. Overall, the performance of the mDSF asymmetric 1-valve configuration for Lo Fire is satisfactory. Negative impacts are confined to higher loads where Hi Fire operation will be used.

Similar trends were observed when comparing the stock symmetric high lift configuration (two valves in high lift mode) and the mDSF asymmetric high charge configuration (one valve in low lift and one valve in high lift). Figure 15 shows the fuel consumption at 1500 rpm and 3000 rpm. The mDSF configuration does show a larger benefit at lower loads

due to more aggressive “Millerization”. At higher loads, however, fuel consumption is worse, and the range is limited as a result of higher boost requirements and knock concerns. This could present a challenge for mDSF acceleration performance and will need to be addressed through further calibration or combustion system optimization. Trends for engine-out noxious emissions are also presented in Figure 16 at 1500 rpm. At higher loads, the mDSF asymmetric strategy showed higher CO and lower NO_x emissions, likely due to reduced combustion efficiency from reduced tumble motion.

FIGURE 15 Comparison of NSFC between high charge stock symmetric and mDSF asymmetric configurations. mDSF showed improvements at low load but worsened at higher loads. Maximum load was also reduced.

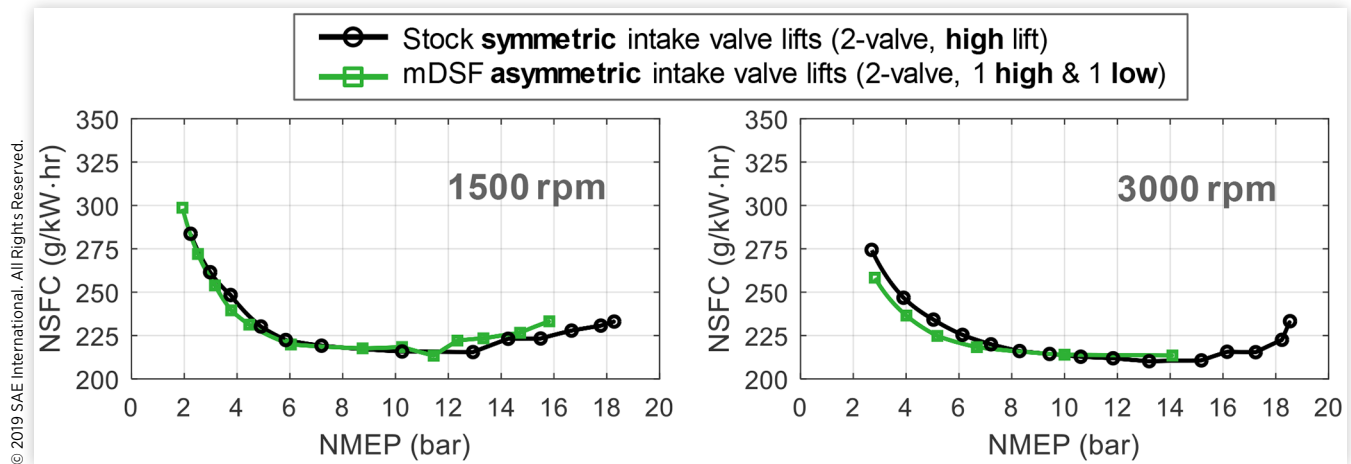
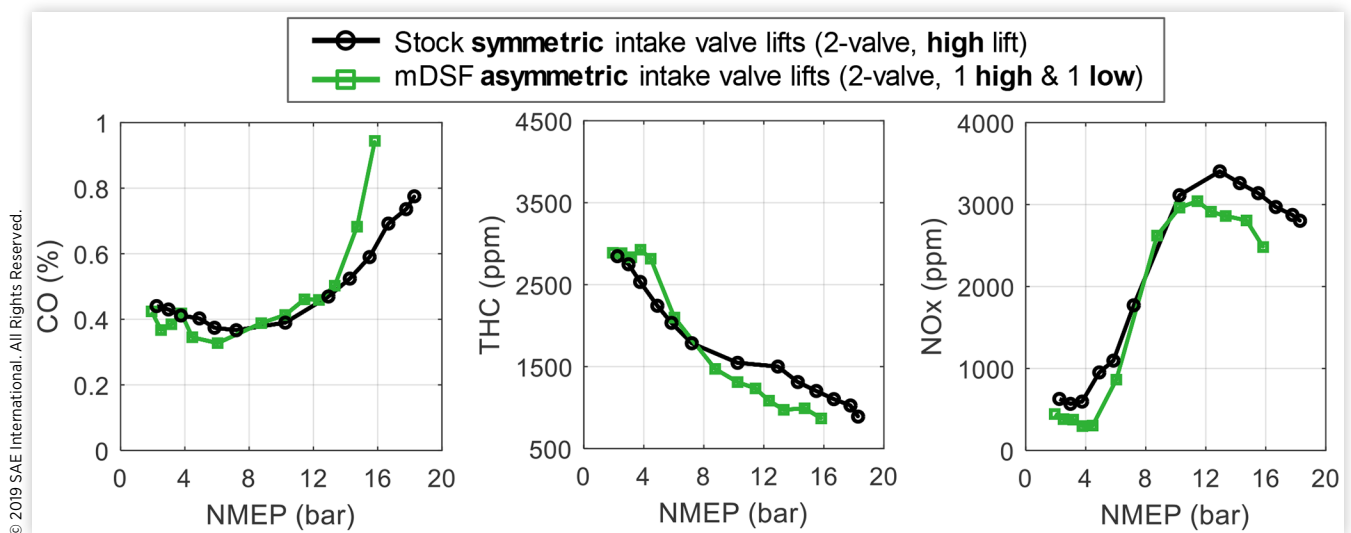


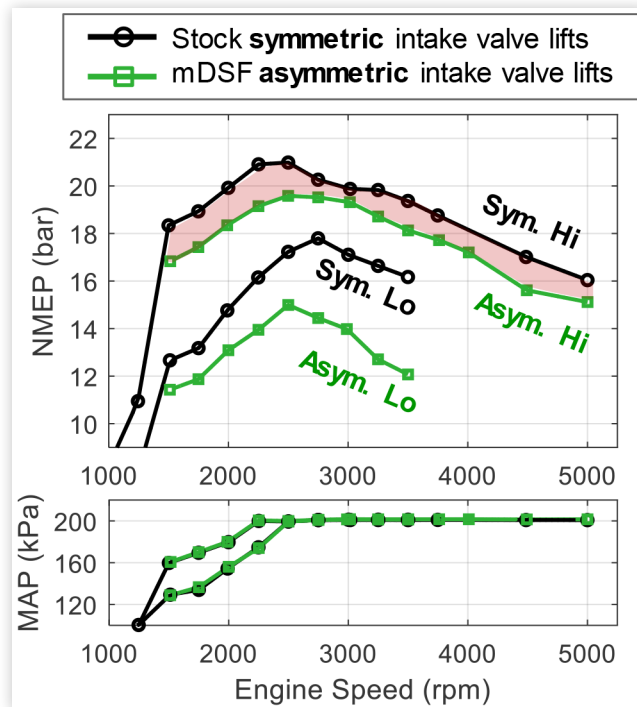
FIGURE 16 Comparison of engine emissions between high charge stock symmetric and mDSF asymmetric intake valve lifts at 1500 rpm. At higher loads, the mDSF strategy shows increased CO and decreased NOx. This is likely a result of lower combustion efficiency from more retarded combustion as a result of disturbed charge motion.



Additional steady-state tests were conducted to compare the high load potential of the two mDSF valve configurations with the stock counterparts across the engine speed range. At each engine speed, tests were carried out at the same manifold pressures for all configurations. Even though MAP and associated loads were high, the tests were not intended to demonstrate maximum torque, but instead illustrate any shortcomings from the asymmetric valve strategies. The results of these high load test are shown in Figure 17. For both the low and high charge, the mDSF asymmetric valve configuration produces lower torque. This is a lesser concern for the lower charge configuration because test data shows the efficiency of the low and high charge modes is very similar at loads above 6 bar. It could also be beneficial to have more charge separation between the Lo Fire and Hi Fire from the

standpoint of NVH. Further, the advanced control algorithms developed for mDSF would enable seamless and frequent transitions between modes, effectively eliminating the issue. The mDSF high charge asymmetric valve configuration presents a bigger challenge since maintaining acceleration performance is one of the requirements for the mDSF technology. The area highlighted in red in Figure 17 shows a 3-8% reduction in torque and is a direct result of the flow area reduction when operating with one high lift and one low lift valve profile. Since upsizing the engine is not necessarily a viable option, Tula is confident the torque loss can be mitigated through optimization of the combustion system, including valve lifts and ports. Increasing the boost pressure by 10-30 kPa with an appropriate turbocharger unit may also provide adequate airflow [23].

FIGURE 17 Comparison of high load torque output between stock symmetric and mDSF asymmetric valve lifts.



Model-Based Combustion Analysis

Each cylinder of the mDSF engine dynamically switches among three operating states: high charge firing with both intake valves operating in combined high-low lift (asymmetric valve lifts), low charge firing with single intake valve running at low lift, and deactivation. Comparing with the stock symmetric intake valve lifts, the in-cylinder air motion will be altered, especially the low-charge firing condition which deactivates one intake valve. In-cylinder charge motion plays a vital role in fuel-air mixing, flame kernel formation, flame propagation, and therefore must be further investigated. In this study, a three-pressure analysis (TPA) model, and a cylinder-pressure-only analysis model (CPOA) were built in GT-SUITE [26] with the aim of quantifying the effect of charge motion.

The TPA model focuses on the analysis of key engine parts, including the intake manifold, intake ports, cylinders and exhaust ports. The rest of the engine systems were replaced by end-environments, where the measured intake manifold and exhaust ports pressures were imposed. The in-cylinder pressure was imposed in the model, and burn rate was iterated at each time step to achieve the measured cylinder pressure.

A matrix of intake port flow tests was conducted with the cylinder head of the EA888 Gen. 3B engine to measure the mass flow rate, swirl, and tumble intensity of every combination of valve lifts in 1 mm increments. The flow coefficients for each valve combination were calculated from the measured mass flow rate. The flow coefficients in the reverse direction were also obtained as they are important to correctly capture the residual gases in the cylinder.

FIGURE 18 Forward flow, reverse flow, tumble, and swirl coefficients for every combination of valve lifts in 1 mm steps (from flow bench measurements of EA888 Gen. 3B cylinder head).

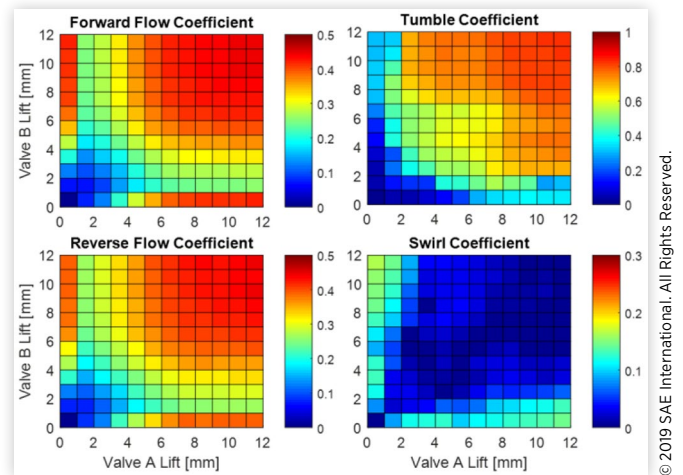


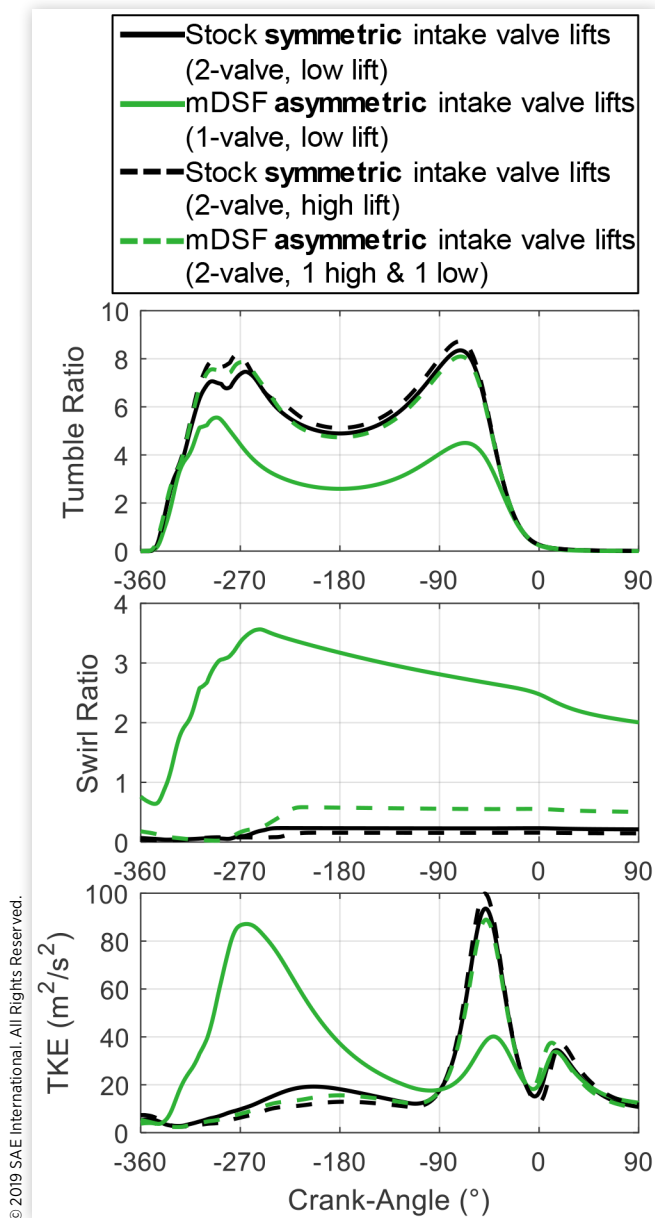
Figure 18 depicts the forward and reverse flow coefficients maps used in the model. As shown in the forward coefficients map, the flow coefficients for single valve operation (valve A lift = 0 or valve B lift = 0) is only reduced by approximately 3% comparing with stock symmetrical valve operation. However, the reverse flow coefficients decreased by about 8% for single-valve operation.

Figure 18 also shows the map of tumble and swirl coefficients from flow bench measurements. The tumble and swirl coefficients define the fraction of the linear momentum entering the cylinder that is converted into angular momentum of swirl and tumble. The combination of swirl and tumble coefficient for each condition is less than 1. The EA888 Gen3B engine is designed to have strong tumble motion; the tumble coefficients are more than 0.8 when both valve lifts are greater than 9 mm. The tumble coefficients are reduced by half for single valve operation (valve A lift = 0 or valve B lift = 0). The swirl is nearly 0 when both valve lifts are higher than 3 mm. However, single valve operation led to increased swirl coefficient of 0.15.

The heat transfer model 'WoschniHuber', which accounts for the impact of in-cylinder air motion on in-cylinder heat transfer, was employed in the TPA and CPOA simulations. In addition, the model was correlated with engine dynamometer test data of 4 engine speeds and 12 engine loads conditions in each of the following operating states: (1) stock low firing with both valves running at low lift, (2) stock high firing with both valves running at high lift, (3) mDSF low (or asymmetric low) firing with single valve opening at low lift, (4) mDSF high (asymmetric high) firing with one valve at high lift and the other valve at low lift.

Figure 19 illustrates the tumble ratio, swirl ratio and turbulent kinetic energy (TKE) as a function of crank-angle degree for each valve configuration at 1500 rpm and 60 kPa intake manifold pressure. Tumble and swirl ratios were defined as the angular velocity of tumble or swirl motion of in-cylinder air divided by the angular velocity of the engine crankshaft. As demonstrated in Figure 19, strong tumble

FIGURE 19 Comparison of tumble ratio, swirl ratio and turbulent kinetic energy for stock and mDSF low firing, stock and mDSF high firing at 1500 rpm, 0.6 bar intake manifold pressure



was formed during inlet with the peak near the middle of the intake stroke (-270°CA aTDC). The strong tumble persisted until the piston approaching TDC causes the large-scale tumble to break up into small-scale turbulence, resulting in intensifying turbulent kinetic energy during compression stroke. Even though the tumble was reduced for the single valve operation (mDSF low firing), similar tumble ratio was achieved late in the compression stroke (after about -30°CA aTDC). Meanwhile, much stronger swirl motion was observed for single valve mDSF operation, with the swirl being maintained during compression as it was less significantly affected by piston motion than tumble. The swirl ratio was around 2 at typical spark timing and during

the combustion process for the mDSF single-valve configuration. Single-valve operation also enhanced the turbulence generated during the intake process, but the turbulence decayed by the middle of the compression stroke and thus would not facilitate faster flame propagation. While the mDSF single-valve configuration had a different evolution of TKE during the cycle due to enhanced swirl and reduced tumble, the combined effect resulted in a similar TKE level between stock and mDSF operations approaching TDC. Similar results were observed at other engine speed and load conditions.

Figure 20 compares the swirl ratio, tumble ratio, and TKE at the spark timing for each valve configuration at 1500 rpm and different intake manifold pressures. Stronger swirl and similar levels of tumble and turbulence were observed for

FIGURE 20 Tumble ratio, swirl ratio, and turbulent kinetic energy at spark timing for 1500 rpm.

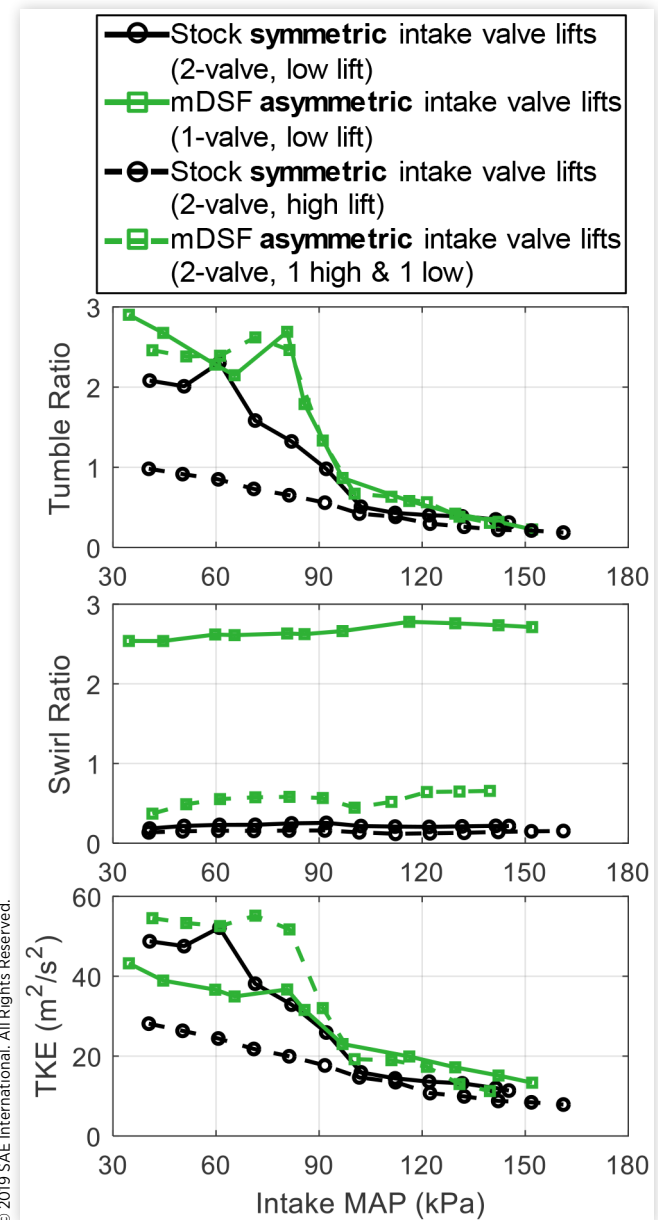
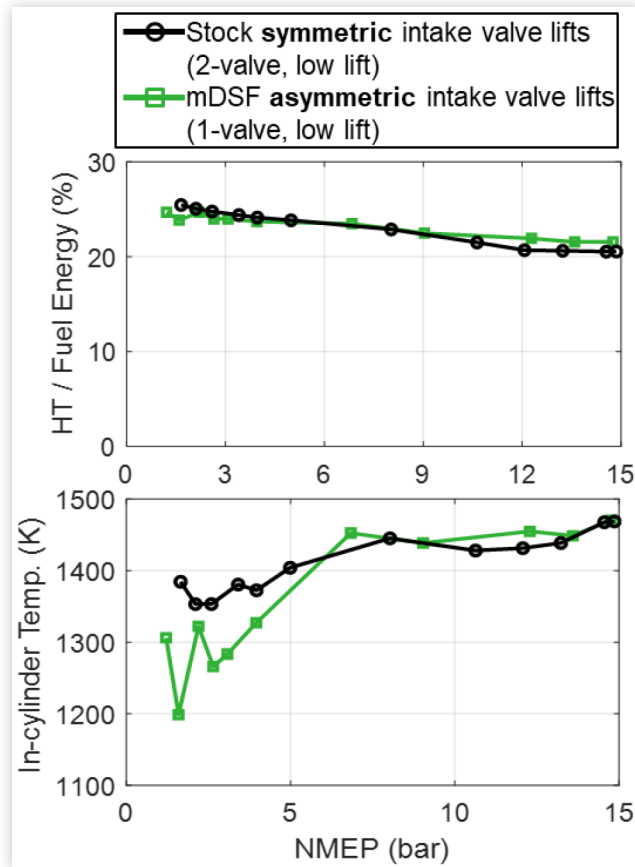


FIGURE 21 Top: the percentage of in-cylinder heat transfer energy in total fuel energy comparison between stock and mDSF low firing operations at 1500 rpm. Bottom: the in-cylinder temperature.



© 2019 SAE International. All Rights Reserved.

stock and mDSF configurations. Therefore, even though mDSF operation altered the in-cylinder flow motion, it did not significantly reduce the turbulence intensity at spark timing, which is critical to the combustion process.

Flow charge motion affects the in-cylinder heat transfer. To quantify the heat transfer effect, a CPOA model, which only includes the engine cylinder, fuel injector, and engine crank train, was developed to remove any potential error from gas exchange simulation in the TPA model. The cylinder initial conditions of the CPOA model, i.e. the residual fraction, trapping ratio, wall temperature, swirl ratio, tumble ratio, and turbulent kinetic energy, were obtained from the TPA simulation. The measured fuel and air flow, as well as the in-cylinder pressure measurements were imposed in the CPOA model.

To better understand the similar NSFC versus NMEP for mDSF low fire and stock low, the total heat transfer energy predicted by the CPOA model was normalized by the total fuel energy and is shown for stock and mDSF low fire configurations at 1500 rpm in Figure 21. The average in-cylinder temperature (from -100 to 180°CAaTDC) is also illustrated in Figure 21. Although the enhanced swirl motion for mDSF low fire increased the in-cylinder heat transfer, the lower average in-cylinder temperature reduced the heat transfer. The competing effects led to similar (within 1% difference in

Figure 21) total heat transfer for stock and mDSF low fire conditions. The lower in-cylinder temperature of mDSF low firing results from the use of a higher intake manifold pressure and different intake cam phasing, which reduces exhaust backflow into the intake manifold. Despite the increased manifold pressure for mDSF low fire, PMEP was very similar to stock low fire (not shown). In addition, spark timing could be further optimized for mDSF low fire as the enhanced swirl motion promoted combustion stability [27, 28]. The combined effects led to similar combustion efficiency and fuel consumption, as shown in Figure 11. It is worth mentioning that the heat transfer rate and combustion efficiency for stock and mDSF high fire configurations were nearly the same (not shown).

Vehicle Fuel Consumption Projections

Vehicle Model and Simulation Methodology

Drive cycle fuel consumption simulations for the baseline EA888 Gen. 3B and mDSF engines were conducted using a previously developed and calibrated vehicle model of Tula's 2015 Volkswagen Jetta demonstrator vehicle [14] in GT-SUITE [29]. The vehicle specifications are listed in Table 2.

Stop-start functionality is assumed in the simulation, although it is not implemented on the demonstration vehicle. This assumption was made to reflect increased adoption of stop-start systems in future vehicles [30]. Road load coefficients were taken from the EPA database [31] and the inertias and mechanical efficiencies of powertrain components were accounted for. The vehicle simulation utilized a driver model controller to follow a desired vehicle speed profile. Gear shifts were dictated by a defined shift schedule from the stock vehicle. To reflect the minimum oil temperature requirement of the hydraulically-actuated deactivation hardware, no cylinder deactivation ($FD < 1$) was permitted until after 100 seconds into cold-start drive cycles.

The engine was modeled using steady-state fuel consumption maps in the vehicle simulation. For the baseline EA888 Gen. 3B, a single fuel consumption map was derived from measured dynamometer data, using reverse engineered engine calibrations from the stock vehicle. For mDSF, a fueling map

TABLE 2 Vehicle specifications for drive cycle simulations.

Vehicle	2015 Volkswagen Jetta SEL
Test Weight	1588 kg
Transmission	6-speed A/T with torque converter clutch
Gear Ratios	4.459, 2.508, 1.556, 1.142, 0.851, 0.672
Final Drive Ratio	3.23
Driven Wheels	Front
Tires	225/45 R17

© 2019 SAE International. All Rights Reserved.

© 2019 SAE International. All Rights Reserved.

was derived from measured dynamometer data for each gear (six maps) depending on the gear-dependent NVH limitations of mDSF. NVH limitations were derived using measured frequency response data from the vehicle with DSF-specific passive driveline hardware mitigation and controlled levels of torque converter clutch (TCC) slip.

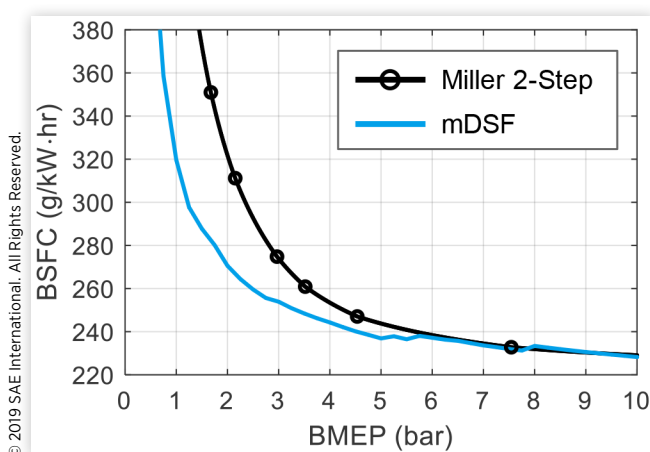
Since only all-cylinder operation was measured on the dynamometer, injection mass was mapped on a cylinder-specific load basis (i.e. NMEP) to use for scaling with FD/HS. That is, an individual firing event was expected to behave the same in mDSF operation as in all-cylinder operation. While this assumption neglects manifold pressure fluctuations and residual gas differences on re-activation after a skip, it has proven to be a reasonable approximation in previous studies [5, 14, 21, 32]. Separate injection mass/NMEP relationships were developed for mDSF low fire and high fire.

The mDSF fueling maps were created by evaluating the fuel consumption of each FD/HS combination that met the NVH limitations at a specified engine speed and load and choosing the FD/HS combination with the lowest fuel consumption. A manifold pressure matching constraint was imposed for mixing mDSF low fires and high fires in the fuel maps. Cam position matching was not enforced since the relative phasing between the two valve lift profiles was not optimized. It is expected that the final implementation of mDSF will include such an optimization.

An example of the fuel consumption derived for mDSF (Gear 6) compared to the baseline Miller 2-Step is presented in Figure 22 as BSFC versus BMEP at 1500 rpm. mDSF provides substantial fuel consumption savings compared to the baseline Miller 2-Step at loads up to 5.5 bar BMEP, including 17% reduction at 2 bar BMEP. Further benefits are expected from implementation of a more aggressive Miller cycle and refinement of NVH characteristics in mDSF operation.

An additional fuel map for mDSF was created for use when mDSF functionality was not enabled (i.e. during the warm up period of a cold-start cycle) containing two possible states: (1) all-cylinder operation with mDSF low fire, and (2) all-cylinder operation with mDSF high fire. The switchover

FIGURE 22 BSFC versus BMEP at 1500 rpm for the baseline Miller 2-Step and mDSF low (Gear 6). mDSF leads to substantial BSFC reductions compared to the baseline Miller 2-Step at BMEP < 5.5 bar.



© 2019 SAE International. All Rights Reserved.

point from mDSF low fire to mDSF high fire was made considering optimal fuel consumption.

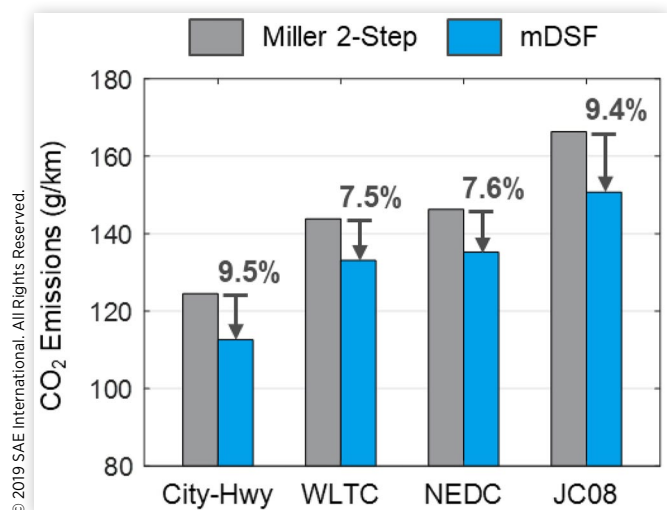
Drive Cycle Fuel Consumption Results

Vehicle simulations were carried out for the US City-Highway (FTP75), WLTC Class 3, NEDC and JC08 drive cycles. The results of the vehicle simulations for the baseline Miller 2-Step engine and the mDSF engine are presented in Figure 23. These projections, based on engine dynamometer data, indicate that mDSF can improve CO₂ emissions by 7.5% to 9.5% from the stock Miller 2-Step engine, which already delivers class-benchmark efficiency. These efficiency gains from mDSF are expected to be even more robust to NVH constraints or sensitive platforms compared with standard DSF and could increase further through optimized engine design that better aligns with the mDSF strategy.

The fuel efficiency gains delivered by mDSF become more impressive when the cost is factored in. Assuming a Miller cycle combustion system is available, the incremental OEM on-cost for mDSF from DSF is very low. In the current configuration, this would consist primarily of four additional OCVs. The mDSF technology, therefore, offers one of the best values for gasoline engine powertrains in the market with relative short-term viability.

To illustrate how mDSF leads to significant CO₂ reduction compared to the baseline Miller 2-Step, BSFC contour maps for each engine are presented in Figure 24 with cycle fuel consumption on the WLTC binned by engine speed/load overlaid as circles (circle radius is proportional to fuel consumption). For mDSF with FD < 1, 40 rpm of TCC slip was used for NVH management such that the engine speed was increased compared to the baseline without TCC slip. For the fuel binning in Figure 24, this has the effect of moving some of the fuel consumption to a higher engine speed bin

FIGURE 23 Baseline and mDSF CO₂ emissions from simulation for four drive cycles: US City-Highway (FTP75/HWFET), WLTC Class 3, NEDC, and JC08. mDSF reduces CO₂ compared the baseline 2-step Miller engine by 7.5-9.5%.



© 2019 SAE International. All Rights Reserved.

FIGURE 24 For the WLTC, fuel consumption overlaid on baseline Miller 2-step BSFC map (top) and mDSF BSFC map in a representative gear (Gear 6, bottom). Cycle fuel consumption was binned by engine speed and torque, with the radius of each circle representing the total fuel consumed in that bin. The maximum engine load curve is denoted by the thick solid black line. Note that mDSF operation with $FD < 1$ utilizes 40 rpm TCC slip, leading to higher engine speed.

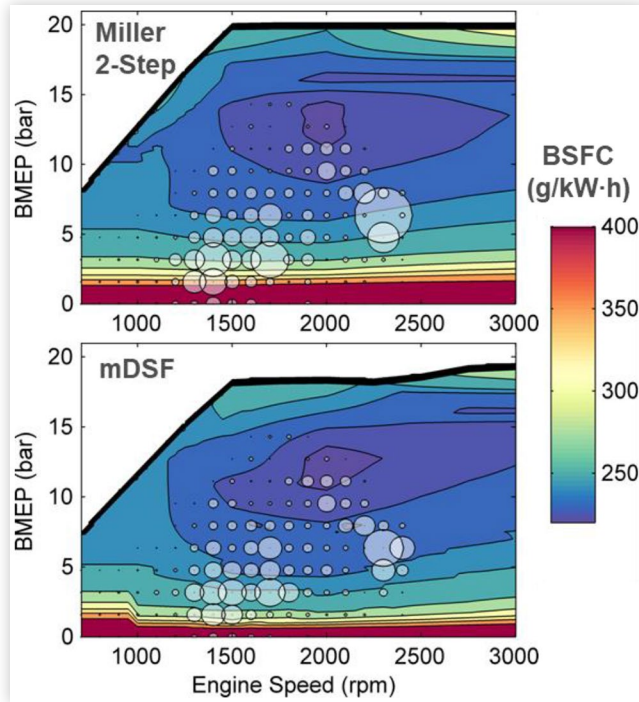
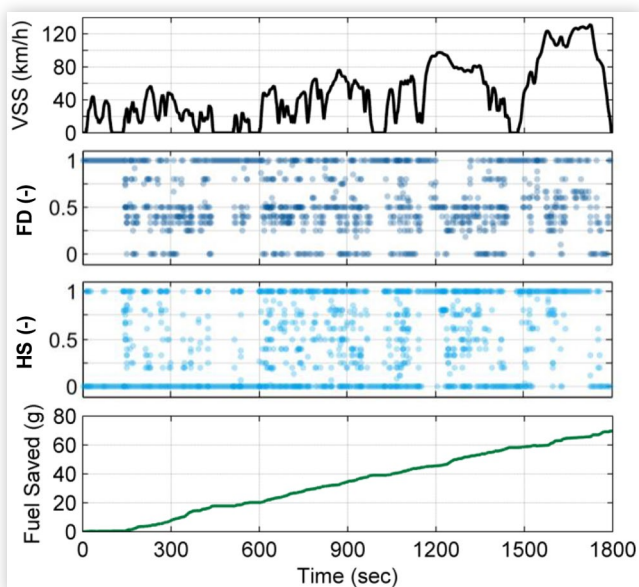


FIGURE 25 Time trace over the WLTC of vehicle speed (VSS), FD, HS, and cumulative fuel saved versus baseline Miller 2-step.



when $FD < 1$. Significant amounts of fuel were consumed below 5 bar BMEP between 1200 - 2000 rpm where mDSF provides significantly improved BSFC. Improved BSFC below 5 bar BMEP can be seen by the BSFC contour levels occurring at lower load compared to the baseline Miller 2-Step.

The fuel consumption savings from mDSF over the WLTC are also illustrated in trace form in Figure 25, which shows the time history of vehicle speed, FD, HS, and the cumulative fuel saved over the baseline Miller 2-Step. On the WLTC, $FD < 1$ was used 53% of the time with 16% of the total cycle time in DCCO. The mixing of high fire and low fire states ($0 < HS < 1$) was utilized during 7% of the cycle time. Utilization of high fire/low fire mixing would increase if the low fire state adopted a more aggressive Miller strategy. The persistent use of $FD < 1$ during the cycle leads to steady accumulation of fuel savings, although the rate of fuel savings was decreased when the engine load was elevated (as expected), such as during acceleration events starting near 1150 seconds or 1480 seconds.

Summary and Conclusions

mDSF is a novel cylinder deactivation technology developed at Tula Technology, which integrates Dynamic Skip Fire (DSF) and Miller cycle engines to deliver maximum fuel consumption improvements at minimal cost. mDSF employs a valvetrain with variable valve lift plus deactivation and novel control algorithms founded on Tula's proven DSF technology. This allows cylinders to dynamically alternate among 3 potential states: high-charge fire, low-charge fire, and skip (deactivation). The low-charge fire state is achieved through an aggressive Miller cycle with Early Intake Valve Closing (EIVC). The three operating states in mDSF can be used to simultaneously optimize engine efficiency and driveline vibrations. Acceleration performance is retained using the all-cylinder, high-charge firing mode. A lower cost valvetrain solution for mDSF is comprised of asymmetric intake valve lifts and/or ports, with one high-flow power charging port and one high-efficiency Miller port. The power charging port is deactivated independently, whereas the Miller port deactivation is coupled to the exhaust valves. High-charge firing is realized with all four valves active, low-charge firing is realized with the power valve deactivated, and skip is realized with all four valves deactivated.

The mDSF asymmetric valve strategy was compared to the baseline symmetric valve strategy through dynamometer tests in a production Miller cycle engine and minimal degradation in efficiency was observed. Maximum torque was reduced by 3-8% for mDSF, but it is expected that this can be recovered with combustion system optimization. Detailed model-based analysis revealed a significant reduction in tumble flow and an increase in swirl motion with the mDSF asymmetric 1-valve low charge configuration, which could potentially lead to longer burn durations and lower combustion stability. This was mitigated in the engine experiments by adjusting spark timing such that combustion phasing and efficiency was maintained. The mDSF 2-valve high charge

configuration did not show noticeable differences in the conditions evaluated.

Engine fuel consumption maps were generated based on experimental data and mDSF “flyzones” were estimated using Tula’s extensive NVH database and experience. Compared with a production state-of-the-art Miller cycle engine baseline, mDSF was projected to reduce fuel consumption by 9.5% in the US City-Highway cycle and 7.5% in the WLTC (Class 3).

Combined with a relatively low added cost of the proposed valvetrain design, mDSF presents an unparalleled cost-benefit ratio in the market with relatively short-term production viability. A fully functional mDSF cylinder head is now operational at Tula’s engine dynamometer and a demonstration vehicle is in development. A combustion system optimization effort is also expected to begin soon.

References

- Sitty, G. and Taft, N., “What Will the Global Light-Duty Vehicle Fleet Look like through 2050?,” 2016.
- Wilcutts, M., Switkes, J., Shost, M., and Tripathi, A., “Design and Benefits of Dynamic Skip Fire Strategies for Cylinder Deactivated Engines,” *SAE Int. J. Engines* 6(1):278-288, 2013, doi:10.4271/2013-01-0359.
- Chien, L.-C., Younkins, M., and Wilcutts, M., “Modeling and Simulation of Airflow Dynamics in a Dynamic Skip Fire Engine,” SAE Technical Paper 2015-01-1717, 2015, doi:10.4271/2015-01-1717.
- Eisazadeh-far, K. and Younkins, M., “Fuel Economy Gains through Dynamic-Skip-Fire in Spark Ignition Engines,” SAE Technical Paper 2016-01-0672, 2016, doi:10.4271/2016-01-0672.
- Younkins, M., Ortiz-Soto, E., Wilcutts, M., Fuerst, J. et al., “Dynamic Skip Fire: New Technologies for Innovative Propulsion Systems,” in *39th International Vienna Motor Symposium*, 2018.
- Fuschetto, J., Eisazadeh-Far, K., Younkins, M., Carlson, S. et al. “Dynamic Skip Fire in Four-Cylinder Spark Ignition Engines: Fuel Economy Gains and Pollutant Emissions Reductions,” in *SAE WCX 2017*, 2017.
- Confer, K.A., Kirwan, J., Delphi, B.F., Younkins, M. et al. “Dynamic Skip Fire Cylinder Deactivation: Application to a 4-Cylinder Turbocharged Vehicle,” in *SAE WCX 2017*, 2017.
- Miller, R., “Supercharged Intercooled Two Stroke Cycle Engine with Compression Control Walve,” 2,991,616, 1961.
- Friedl, H., “Trends & Drivers for Passenger Car Powertrain Technology,” in *Mahindra AFS Technology Symposium*, 2016.
- Anderson, M.K., Assanis, D.N., and Filipi, Z., “First and Second Law Analyses of a Naturally-Aspirated, Miller Cycle, SI Engine with Late Intake Valve Closure,” SAE Technical Paper 980889, 1998, doi:10.4271/980889.
- Li, T., Gao, Y., Wang, J., and Chen, Z., “The Miller Cycle Effects on Improvement of Fuel Economy in a Highly Boosted, High Compression Ratio, Direct-Injection Gasoline Engine: EIVC Vs. LIVC,” *Energy Convers. Manag.* 79, 2014.
- Kapus, P., Prevedel, K., Wolkerstorfer, J., and Neubauer, M., “200 g / kWh - Can the Stoichiometric Gasoline Engine Beat the Diesel ?” *22nd Aachen Colloq. Automob. Engine Technol*1031-1050, 2013.
- Budack, R., Wurms, R., Mendl, G., and Heiduk, T., “The New Audi 2.0-L I4 TFSI Engine,” *MTZ* 77(5):16-23, 2016.
- Wilcutts, M., Nagashima, M., Eisazadeh-far, K., Younkins, M. et al., “Electrified Dynamic Skip Fire (eDSF): Design and Benefits,” SAE Technical Paper 2018-01-0864, 2018, doi:10.4271/2018-01-0864.
- Ortiz-Soto, E., Wang, R., Nagashima, M., Younkins, M. et al., “λ DSF: Dynamic Skip Fire with Homogeneous Lean Burn for Improved Fuel Consumption, Emissions and Drivability,” SAE Technical Paper 2018-01-0891, 2018, doi:10.4271/2018-01-0891.
- Chen S.K., Wang R., Younkins M., Scassa M. et al. “Dynamic Skip Fire Applied to a Diesel Engine for Improved Fuel Consumption and Emissions,” in *4th International FEV Conference on Diesel Powertrains 3.0*, 2018.
- Ram S., Serrano L.J., and Younkins M.A., “Autonomous Driving with Dynamic Skip Fire,” US9983583B2, 08-Aug-2017.
- Haas M., “Just Air? UniAir - The First Fully-Variable, Electro-Hydraulic Valve Control System,” 2010.
- Luttermann, C., Schünemann, E., and Klauer, N., “Enhanced VALVETRONIC Technology for Meeting SULEV Emission Requirements,” 2006.
- Sherman, D., “All-New Four-Cylinder for 2019 Chevrolet Silverado,” *Automotive Engineering*, 2018. [Online] <https://www.sae.org/news/2018/05/gm-2.7-l-i-4-revealed>, accessed Oct. 31, 2018.
- Younkins, M., Fuerst, J., Carlson, S., Kirwan, J. et al., “Dynamic Skip Fire: The Ultimate Cylinder Deactivation Strategy,” in *38th International Vienna Motor Symposium*, 2017.
- Moore, W., Foster, M., Lai, M.-C., Xie, X.-B. et al., “Charge Motion Benefits of Valve Deactivation to Reduce Fuel Consumption and Emissions in a GDi, VVA Engine,” SAE Technical Paper 2011-01-1221, 2011, doi:10.4271/2011-01-1221.
- Medicke, M., Günther, M., and Brenner, A., “Charge Motion Concepts for Modern Combustion Processes,” in *Gas Exchange Conference*, 2017.
- Bowyer, S., Chandler, C., de Bruijn, R., and Ortiz-Soto, E., “Cylinder Head Design to Operate Using mDSF,” SAE Technical Paper 19PFL-0758.
- “Patents - Tula Technology.” [Online] <https://www.tulatech.com/patents/>, accessed: Jun. 28, 2018.
- “GT-SUITE Version 2018,” Gamma Technologies, Westmont, IL, 2018.
- Chen, H., Xu, M., Hung, D.L.S., and Zhuang, H., “Cycle-To-Cycle Variation Analysis of Early Flame Propagation in Engine Cylinder Using Proper Orthogonal Decomposition,” *Exp. Therm. Fluid Sci.* 58:48-55, 2014.
- Hung, D.L.S., Chen, H., Xu, M., Yang, J. et al., “Experimental Investigation of the Variations of Early Flame Development in a Spark-Ignition Direct-Injection Optical Engine,” in

Volume 1: Large Bore Engines; Advanced Combustion; Emissions Control Systems; Instrumentation, Controls, and Hybrids, 2013, V001T03A010.

29. "GT-SUITE Version 7.5," Gamma Technologies, Westmont, IL, 2016.
30. Wolfram, P., German, J., Mock, P., and Tietge, U., "Deployment of Passenger Car Technology in Europe and the United States," Washington, DC, 2016.
31. EPA, "Data on Cars Used for Testing Fuel Economy." [Online] <https://www.epa.gov/sites/production/files/2016-07/15ststcar.csv>, accessed Aug. 20, 2010.
32. Younkins, M., Ortiz-Soto, E., Wilcutts, M., and Fuerst, J., "Advances in Dynamic Skip Fire : eDSF and mDSF," *Aachen Colloq. Automob. Engine Technol.*1-26, 2018.

Contact Information

Elliott Ortiz-Soto, Ph.D.
ortizsotoe@tulatech.com
 (408) 708-7534

Acknowledgments

The authors would like to acknowledge members of the Tula team Changhoon Oh, Joel Van Ess and Jerry Fuschetto for their efforts on reverse engineering, controls development and engine calibration. Ian Ren and Anastasios Arvanitis also provided key support on NVH analysis. The authors would further like to recognize Chris Chandler, Casey Horner, Darin Zimlinghaus and Alex Perry for their vital role in building, integrating and testing the mDSF engine on Tula's dynamometer, as well as Jack Parsels, Jack Lehnert and Steve Niederer for the engine wiring harness, dSPACE hardware and instrumentation.

Definitions/Abbreviations

A/T - Automatic transmission (w/ torque converter)
aTDC - After top dead center (compression)

BMEP - Brake mean effective pressure
BSFC - Brake specific fuel consumption
bTDC - Before top dead center (compression)
C - mDSF low-to-high charge ratio
CA - Crank angle
CAFE - Corporate Average Fuel Economy (U.S.)
COV - Coefficient of variation
DCCO - Deceleration cylinder cut-off
DFCO - Deceleration fuel cut-off
dRFF - Deactivatable roller finger follower
DSF - Dynamic Skip Fire
eFD - Effective firing density (mDSF)
FD - Firing density
FFT - Fast Fourier transform
FTP - Federal Test Cycle (U.S.)
HS - mDSF Hi Fire share (Hi Fire / Total Fires)
HLA - Hydraulic lash adjuster
HWFET - EPA Highway Fuel Economy Test Cycle (U.S.)
NEDC - New European Driving Cycle
NMEP - Net indicated mean effective pressure (720° CA)
NSFC - Net indicated specific fuel consumption (720° CA)
NVH - Noise, vibration and harshness
OCV - Oil control valve
RDE - Real Driving Emissions
RON - Research octane number
SI - Spark ignition
TCC - Torque converter clutch
TGDI - Turbocharged, gasoline, direct-injection
TKE - Turbulent kinetic energy
TWC - Three-way catalyst
WLTC - Worldwide Harmonized Light-Duty Vehicles Test Cycle